

# A Novel Method for RF Tomography and Acquiring Dielectric Signatures for Security Applications

Tim Cargol  
Spectrohm, Inc.  
Tysons Corner, VA 22102  
tcargol@spectrohm.com

Scott Teare  
Senior Member, IEEE  
New Mexico Institute of Mining and Technology  
Socorro, NM 87801  
scott.teare@nmt.edu

**Abstract**—Quickly imaging and discriminating materials is becoming increasingly important for security screening. Conventional techniques are effective, but their results can be difficult to interpret when screening for low- $z$  energetic materials such as explosives. In this paper, we present a novel method to identify the distinct signatures that many dielectric materials—potentially including energetic materials—exhibit when excited under radio frequency wavelengths. This novel system combines the ability to penetrate objects with lower-frequency radio waves while achieving a resolution potential traditionally reserved for millimeter waves or X-rays. The system measures impedance changes along a transmission line, generating data on the composition and location of materials in an object under study. This data can be stitched together to form an image via a “transmission line tomography.” A prototype system detected a volume of water concealed within a block of paraffin wax—both low- $z$  materials. The detection system requires no moving parts and can utilize low-cost electronics to move the signals to the analysis computer.

**Keywords**—dielectrics, electromagnetic waves, TE, TEM, through-barrier imaging, propagation velocity, low- $Z$ , energetic materials, transmission line tomography

## I. INTRODUCTION

Rapid evaluation and identification of materials using through-barrier detection techniques is becoming increasingly important as a first-line defense at entry points into countries, buildings, and vehicles and for screening of people, body cavities, and small articles. Conventional techniques using X-ray imaging are effective, but they rely on contrast between materials or energy backscatter for analysis, and their results can be difficult to interpret when attempting to detect low- $Z$  energetic materials such as explosives. These conventional imaging techniques also rely on detecting a recognizable shape, rather than the signature of a substance. Many dielectric materials—potentially including energetic materials—exhibit detectable signatures when excited under radio frequency wavelengths [1]. These unique dielectric signatures can convey a wealth of diagnostic information with applications for security, medicine, manufacturing and other fields. For example, unique dielectric characteristics could be used to distinguish between energetic materials and foodstuffs, or to discriminate among different kinds of biological tissues.

The analysis and determination of a material’s dielectric properties, and, in particular, the spatial resolution of those properties, has traditionally depended on the frequency of the excitation wave. Providing human-scale resolution—for example, to detect explosives concealed under clothing—has required wavelengths under 1 cm [2] [3]. The skin depth of these short wavelengths in lossy materials, however, significantly limits the degree to which they can penetrate objects and precludes measuring the lower-frequency dielectric signatures that arise from materials’ molecular and orientational behaviors.

The behavior of electromagnetic waves in dielectrics has been traditionally analyzed on one of two regimes—low-frequency, or static; and higher-frequency, or ray-like—according to the size of the wavelength relative to the structure under study.

- In static conditions—or where wavelengths are an order of magnitude or more longer than the dielectric structures under investigation—the impedance characteristics of the subject under study will determine the paths of the current. Fields will be drawn into the material of lowest impedance.
- As the frequency increases, however, propagation will take on more ray-like behaviors. Propagation will be dominated by the material of highest propagation velocity.

Low-frequency or static regimes, such as electrical impedance tomography (EIT) or electrical capacitance tomography (ECT), suffer bending and curving of electrical fields as they are drawn into materials of lower impedance. This has earned these techniques the name “soft field” tomography. These low-frequency or static fields can greatly obscure internal detail because they tend to smooth out at appreciable distance from a dielectric structure.

Techniques used at much higher frequencies, such as microwave tomography (MWT), typically use wavelengths smaller than the size of the dielectric structures under study. These wavelengths behave with ray-like or “hard field” characteristics. When materials’ skin depth permits internal propagation of these shorter wavelengths, the shorter

wavelengths are better able to resolve structures. But in most scenarios, the shorter wavelengths also dramatically diffract, reflect, and scatter around structures, which complicates analysis.

In both regimes, solving the inverse problem to reconstruct a tomographic image can be mathematically intractable, either due to the curvature of soft fields or to the scattering of ray-like microwaves.

Thus, an ideal electromagnetic tomography system would combine the penetration of lower-frequency soft-field techniques, but with the ray-like linearity or hard-field characteristics of higher frequencies.

## II. ELICITING HARD FIELD BEHAVIOR FROM SOFT FIELDS

A wave propagating in transverse electric (TE) or transverse electric and magnetic (TEM) modes is comprised of electric fields orthogonal to the direction of propagation. Therefore, if an electromagnetic wave is propagating in a known direction and its propagation is determined to be in TE or TEM mode, linearity and direction of its electric fields can be assumed.

In TE or TEM modes propagating through a dielectric medium, the velocity of propagation ( $V_{prop}$ ) and impedance ( $Z$ ) are both related to the media's relative permittivity or dielectric constant ( $\epsilon_r$ ) as a component of its electric permittivity ( $\epsilon = \epsilon_r \epsilon_0$ ), such that:

$$\text{Impedance}(Z) = \sqrt{\frac{\mu}{\epsilon}} \quad V_{prop} = \frac{1}{\sqrt{\epsilon\mu}} \quad V_{prop} = \frac{1}{\epsilon Z} \quad (1)$$

where  $\mu$  is the material's magnetic permeability and  $\epsilon_0$  is the permittivity of free space. The above relationship holds in TE transmission in an inhomogeneous dielectric comprised of structures that are sufficiently small relative to the probing wavelength (or whose traversal time comprises an insignificant fraction of the probing frequency's period) that the dielectric behaves as a mixture or composite dielectric with linear contributions from the constituent dielectrics. These mixtures may have various formulations, but most commonly as:

$$\epsilon_{eff} = \epsilon_1 \left( \frac{\epsilon_2}{\epsilon_2 - f_2(\epsilon_2 - \epsilon_1)} \right) \quad (2)$$

where  $\epsilon_{eff}$  is the effective dielectric constant of a mixture comprised of a first material with dielectric constant  $\epsilon_1$  and a second material of dielectric constant  $\epsilon_2$  comprising  $f_2$  volume fraction of the mixture [4].

In an inhomogeneous dielectric with larger structures, speed and impedance may be dominated by the  $\epsilon_r$  of certain constituent physical elements of the structure. An illustrative example of this phenomenon can be found in commercial coaxial transmission line cables. Consider a foamed polyethylene (PE) coaxial cable such as RG-59: the dielectric is composed of a mixture of PE and microscopic air bubbles, creating a transmission line of 75 Ohms and propagation velocity ( $V_{prop}$ ) of 83% the speed of light. If the same RG-59 cable structure contained the same volume of air and PE, but with the dielectric materials separated into macroscopic regions of pure PE and pure air, these separate regions would have

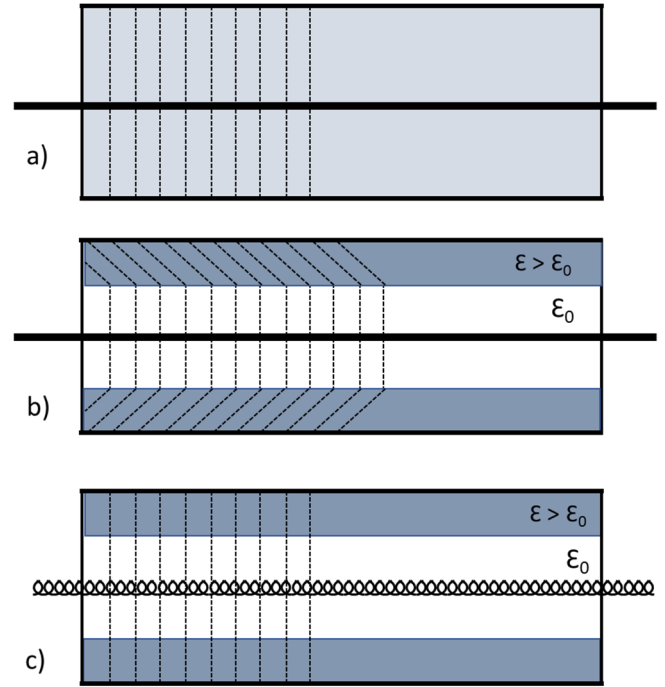


Figure 1: Cross section of notional coaxial cables with dotted lines representing electric field distribution as a wave travels from left to right in a) cable with microscopically mixed dielectric propagating in TEM mode, b) cable with macroscopic bifurcation of constituent dielectrics into axial regions, and c) bifurcated dielectric with inductively loaded center conductor propagating in a TE-like mode.

characteristics of 60 Ohms and 66%  $V_{prop}$  for pure PE and 90 Ohms and 99%  $V_{prop}$  for air [5]. If these bifurcated regions were aligned along the direction of propagation, the differing propagation velocities would disrupt TEM behavior and the wave would behave in a non-uniform fashion and encounter significant dispersion between the slower and faster dielectric components. From a measurement perspective, the line's impedance and propagation velocity (and composite  $\epsilon_{eff}$ ) would be a complex function of the operating frequencies and the PE and air constituent geometries, precluding inverse determination of the line's  $\epsilon_{eff}$ .

If TE mode could be restored to the bifurcated cable, the effective dielectric constant  $\epsilon_{eff}$  could again become a linear function of the fraction of the constituent components such as (2). This can be accomplished by inductively loading the center conductor of the coaxial cable to slow its velocity to match the slower PE constituent as shown in Fig. 1. For example, if instead of the free space relations between propagation velocity and impedance of (1), we consider the lumped element or per-unit-length constructions used for transmission lines:

$$Z_{tl} = \sqrt{\frac{L_{tl}}{C_{tl}}} \quad V_{prop_{tl}} = \frac{1}{\sqrt{L_{tl}C_{tl}}} \quad V_{prop_{tl}} = \frac{1}{\epsilon_{eff}Z_{tl}} \quad (3)$$

where  $L_{tl}$  is the per unit length inductance and  $C_{tl}$  is the per unit length capacitance as a function of  $\epsilon_{eff}$ . Adding a known series inductance  $L_s$  such that  $L_{tl} = L_{tl0} + L_s$  will proportionally slow the  $V_{prop_{tl}}$  while increasing the impedance ( $Z_{tl}$ ) for a transmission line cable operating in TE mode. If, however, the

operating mode was causing a non-representative  $\epsilon_{\text{eff}}$  as shown in Fig. 1 b), the relationship (3) between  $V_{\text{prop}it}$  and  $Z_{it}$  will not hold.

A coaxial cable, like any transmission line, by its nature determines the direction of electric field propagation. And if—as described above—it can be determined that the transmission line is propagating in a TE-like mode, propagating fields’ direction and linearity can be assumed to greatly simplify dielectric measurements of local regions.

### III. FROM TRANSMISSION LINE TO IMAGE RASTER

Voltage and/or current can be measured at points along the length of a transmission line to reveal local changes in line impedance. These impedance changes can be used to calculate a local  $\epsilon_{\text{eff}}$ . Local propagation velocity from point to point can be likewise measured and used to derive an  $\epsilon_{\text{eff}}$ . Comparing the impedance-derived and velocity-derived  $\epsilon_{\text{eff}}$  will indicate whether a TE-like mode is present, and the line’s inductance can be adjusted to find or verify TE-like mode.

If the propagation speed is faster than local  $\epsilon_{\text{eff}}$ , measured impedance will increase because the fields will not have time to fully interact with the slower, low-impedance dielectric components. Likewise, if the speed of propagation is too slow through a given measurement point, local impedance will also increase, because the fields from previous points will race out ahead and undercut into the area being measured, screening field interaction.

Once accurate  $\epsilon_{\text{eff}}$  data is determined for each measurement point, a representative pixel for each measurement point can be arrayed in a line to form a raster. Many such transmission line “rasters” can be arrayed in parallel to form an image by either panning the line over an object for study or placing the object within an array of parallel transmission lines as shown in Fig. 2. Thus, data from multiple measurement points along multiple lines can be stitched together to form an image via a transmission line tomography.

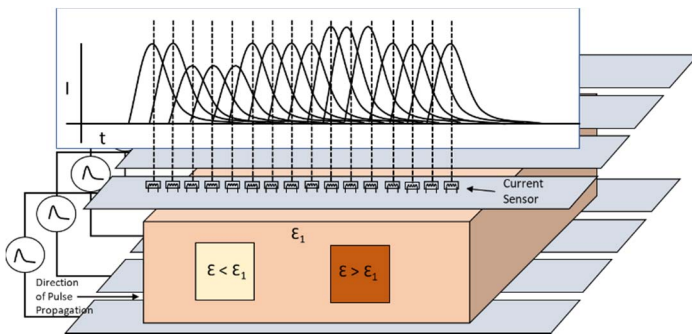


Figure 2: Measurement of impedance changes along a single transmission line among an array of transmission lines spanning a specimen for study.

### IV. APPARATUS

A prototype transmission line tomography system has been developed for the purpose of demonstrating the technique. The system consists of a single, inductively loaded parallel plate transmission line with 48 measurement points spaced at 6mm intervals along its length. The spacing between the transmission line elements is approximately 8 cm and a 7 cm x 16 cm specimen block is inserted between the elements—leaving an approximately 1 cm air gap between the specimen and the top line element as shown in Fig. 3.

The first specimen block is solid paraffin wax composed of light, low-z elements, such as those in energetic materials, typically hydrocarbon molecules. An approximately 3 nS-wide pulse is applied at one end and pulse voltage measured at each of the 48 points. The pulse profile for the solid wax block is shown in Fig. 2. The second test case uses a paraffin wax block of the same profile, but enclosing an 8 cm-wide water cavity—again, both low-Z materials. The pulse pattern from this test is dramatically different from the pattern from the solid block of wax, which demonstrates the sensitivity of the system even when imaging materials composed of light, low-z elements.

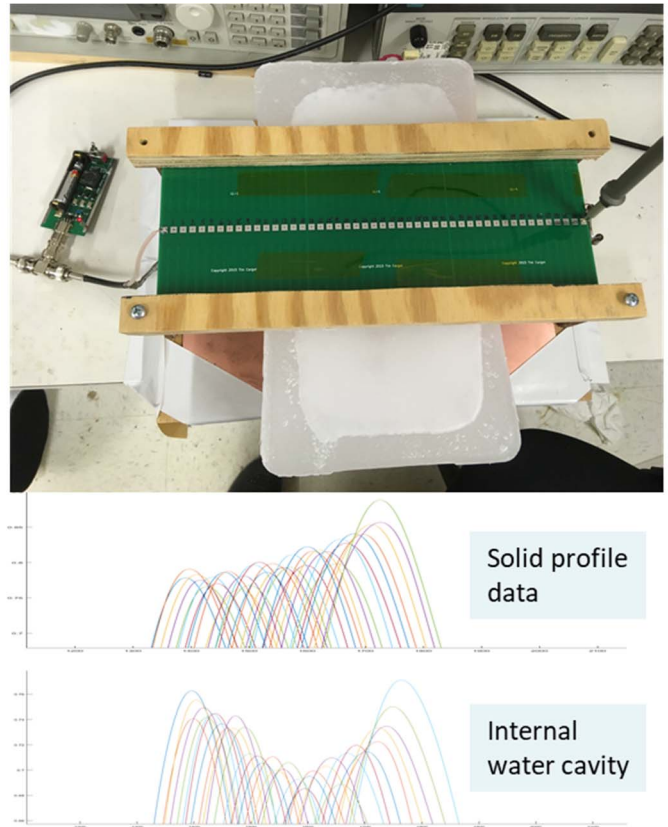


Figure 3: Top: Prototype of detector system being used to interrogate low-Z materials; Bottom: Pulse heights obtained from two low-Z specimens for comparison.

While the prototype system demonstrates the sensitivity of the technique in simple, 1-dimensional material detection scenarios, a more advanced system is being developed to provide spatial resolution in addition to material detection.

Computer models using the package OpenEMS [6] demonstrate more sophisticated imaging and discrimination capabilities. Fig. 4 shows a simulated transmission line tomography system determining the position of air and water voids concealed within a plastic substrate. Notice that there is a clear difference between water and air, as well as between those materials and the plastic substrate. In this simulation, a virtual plastic object of thickness 6 cm is placed between 48 parallel transmission lines of 7 cm spacing and 6 mm width. There is an 8 mm air space between the virtual plastic block and transmission line structures to mimic a real-world standoff.

Each square pixel in Fig. 4 represents data acquired at 6 mm points along the 6 mm-wide lines, making the letters approximately 60 mm x 50 mm, with an overall object size of 280 mm x 280 mm.

This novel approach to imaging dielectric signatures has been demonstrated on small scale, detecting a volume of water concealed within a wax block. The transition to physically larger applications requires increasing the detection region in size and adapting the sensor enclosure to support operational requirements.

The detection system requires no moving parts and can utilize low-cost electronics to move the signals to the analysis computer. Successful detection of contraband will depend on developing a library of specific RF characteristics for materials of interest, in particular energetic materials and contraband.

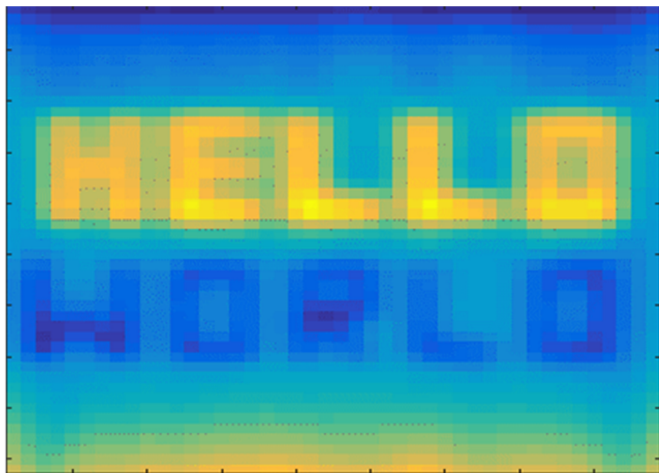


Figure 4: Computer simulation of imaging performance of system, detecting “hello”-shaped air void and “world”-shaped water void within a plastic substrate.

## REFERENCES

- [1] A. R. V. Hippel, Dielectric Materials and Applications, Boston: Artech House, 1995.
- [2] P. K. D. S. a. T. H. D. McMakin, "Dual-surface dielectric depth detector for holographic millimeter-wave security scanners," Proceedings of SPIE, vol. 7309, May 2009.
- [3] J. B. a. B. S. J. Weatherall, "Spectral Signatures for Identifying Explosives With Wideband Millimeter-Wave Illumination," IEEE Trans. Microw. Theory Techn., vol. 64, no. 3, pp. 999-1004, March 2016.
- [4] A. Sihvola, "Self-Consistency Aspects of Dielectric Mixing Theories," IEEE Trans. Geosci. Remote Sensing, vol. 27, no. 4, pp. 403-415, 1989.
- [5] J. K. L. Shen, Applied Electromagnetism, Boston: PWS Publishing Company, 1995, p. 158.
- [6] T. Liebig, openEMS - Open Electromagnetic Field Solver, General and Theoretical Electrical Engineering (ATE), University of Duisburg-Essen.

**Tim Cargol** earned his B.S and M.Eng. degrees in electrical engineering from MIT and conducted extensive research on dielectric materials at MIT’s High Voltage Research Lab before pursuing entrepreneurial opportunities in dielectrics and transmission line-based technologies. He holds 3 patents on dielectric measurement and transmission line technologies.

**Scott Teare** received his PhD in Physics from the University of Guelph, Canada, and is professor of electrical engineering at New Mexico Institute of Mining and Technology in Socorro, NM. He is an active researcher in the areas of optics and the electromagnetic properties of energetic materials. He has more than 100 technical publications and has authored 4 US patents and several books with SPIE Press.